Correspondence and
requests for materials
should be addressed to
B.N. (nbalaji@iastate.
edu) or M.J.W.
(mjwannem@iastate.
edu)

* These authors
contributed equally to
this work.

† Current address:
Boehringer Ingelheim,
Ames, IA 50010.

A systems approach to designing next generation vaccines: combining α-galactose modified antigens with nanoparticle platforms

Yashdeep Phanse[1]*, Brenda R. Carrillo-Conde[2]*, Amanda E. Ramer-Tait[1,5], Scott Broderick[3], Chang Sun Kong[3], Krishna Rajan[3], Ramon Flick[4], Robert B. Mandell[4]†, Balaji Narasimhan[2] & Michael J. Wannemuehler[1]

[1]Department of Veterinary Microbiology and Preventive Medicine, Iowa State University, Ames, IA 50011, [2]Department of Chemical and Biological Engineering, Iowa State University, Ames, IA 50011, [3]Department of Materials Science and Engineering, Iowa State University, Ames, IA 50011, [4]BioProtection Systems Corporation, a subsidiary of NewLink Genetics Corporation, Ames, IA 50010, [5]Department of Food Science and Technology, University of Nebraska-Lincoln, Lincoln, NE 68583.

Innovative vaccine platforms are needed to develop effective countermeasures against emerging and re-emerging diseases. These platforms should direct antigen internalization by antigen presenting cells and promote immunogenic responses. This work describes an innovative systems approach combining two novel platforms, αGalactose (αGal)-modification of antigens and amphiphilic polyanhydride nanoparticles as vaccine delivery vehicles, to rationally design vaccine formulations. Regimens comprising soluble αGal-modified antigen and nanoparticle-encapsulated unmodified antigen induced a high titer, high avidity antibody response with broader epitope recognition of antigenic peptides than other regimen. Proliferation of antigen-specific CD4$^+$ T cells was also enhanced compared to a traditional adjuvant. Combining the technology platforms and augmenting immune response studies with peptide arrays and informatics analysis provides a new paradigm for rational, systems-based design of next generation vaccine platforms against emerging and re-emerging pathogens.

M edical needs have changed considerably in the 21st century due, in part, to the fact that many pathogens have evolved to evade the host immune response. This evolution has rendered current vaccine strategies inadequate for providing protection against emerging and re-emerging infections. Efficient priming of the immune system is required for the induction of robust immune responses. Current vaccines are often less immunostimulatory because soluble doses of antigens are rapidly cleared and poorly immunogenic. Chemical modification of antigens that would target immune cells and/or increase their recognition by immune cells would be important for the induction of protective immunity. Another approach to efficiently prime the immune system is to use adjuvants[1]. Ideally, adjuvants will also function as delivery platforms that can release stable immunogens to antigen presenting cells (APCs) upon immunization. The sustained release of antigen provides for longer and efficient antigen dosing and may ultimately lead to development of single dose vaccines[2]. Conventional approaches in vaccine design in which antigens and off-the-shelf adjuvants are "mixed and matched," have proven to be inefficient. In order to rationally design vaccines and make transformative improvements in vaccine efficacy, it is important to concomitantly design both the antigen and the adjuvant. This work describes a novel systems approach in which the advantage of judiciously combining antigens and nanoscale adjuvants results in the induction of robust immune responses.

Biodegradable polymer-based nanoparticle platforms have been studied extensively for vaccine delivery; specifically, polyanhydride particles possess intrinsic adjuvant properties and have demonstrated the ability to provide sustained release of protein antigens, activate APCs, and modulate the immune response[3–12]. We recently demonstrated the ability of a rationally-designed nanovaccine based on the antigen, F1-V, and amphiphilic nanoparticles composed of 1,6-bis(*p*-carboxyphenoxy)hexane (CPH) and 1,8-bis(*p*-carboxyphenoxy)-3,6-dioxaoctane (CPTEG) to induce long-lived protection (i.e., 280 days after a single intranasal dose) against plague in mice upon lethal challenge with *Yersinia pestis*[11,12].

In this work, we exploit the presence of naturally occurring serum antibody to αGal in order to enhance the humoral response to F1-V, a fusion protein that has been previously utilized as an immunogen in *Y. pestis* vaccines[13]. This was accomplished by haptenating F1-V with αGal epitopes [galactose-alpha(1,3)-galactose-beta(1,4)N-acetylglu-cosamine-R (Gal-α(1,3)-Gal-β(1,4)-GlcNAc-R)]. This approach takes advantage of the absence of α-1,3 galactosyl transferase genes in humans who, therefore, are unable to functionally glycosylate proteins and glycolipids with αGal epitopes[14,15]. Consequently, αGal epitopes found on bacteria and foods are recognized as foreign resulting in the generation of serum anti-αGal antibodies that represent more than 1% of total serum IgG[14,15]. These anti-αGal antibodies can be exploited to target and enhance the interaction of immune complexes (ICs) to follicular dendritic cells and B cells[16–18]. αGal modification has been shown to substantially increase the immunogenicity of proteins as diverse as bovine serum albumin[19] and HIV gp120[18].

Herein, we describe a systems approach by combining αGal modification of F1-V with the amphiphilic polyanhydride nanovaccine platform to rationally design a next generation vaccine against *Y. pestis*. We hypothesize that a systems approach would synergistically augment and accelerate an antigen-specific immune response that recognizes a broader repertoire of antigenic epitopes and allows for the development of a single-dose vaccine that reduces the need for multiple injections. Vaccine formulations composed of these technology platforms were tested in an α1, 3 galactosyltransferase (α1,3GT) gene knockout (KO) mouse model, which lacks αGal epitopes and can produce high-titer anti-αGal antibodies similar to humans, thereby mimicking human immune characteristics[20].

Results

Soluble αGal-F1-V and unmodified F1-V encapsulated within nanoparticles ($S_{αGal} + E_{unmod}$) synergistically generated a high titer, high avidity antibody response. We hypothesized that vaccine formulations consisting of soluble and nanoparticle-encapsulated protein would induce high titer serum antibody, which is generally required to induce protection against several diseases, including plague[21–23]. To test this hypothesis, mice were vaccinated subcutaneously with the vaccine formulations shown in Table 1 and then subcutaneously boosted with 5 μg of unmodified F1-V antigen 37 days after the primary vaccination. Monophosphoryl lipid A (MPLA) is a vaccine adjuvant that has been approved for use in humans by the U.S. Food and Drug Administration (FDA) and was used as a control adjuvant in these studies. Anti-F1-V antibody titers were evaluated pre-boost (day 36) and post-boost (day 42).

The vaccine regimen comprised of soluble αGal-F1-V and nanoparticles encapsulating unmodified F1-V ($S_{αGal} + E_{unmod}$) elicited a high titer, high avidity antibody response against F1-V (Figure 1). Immunizing mice with only unmodified antigen encapsulated in 50 : 50 CPTEG : CPH nanoparticles (i.e., no soluble dose) generated low (<1,000) antibody titers (data not shown). These data indicate that a combination of nanoparticle-encapsulated and soluble antigen is critical for the induction of high antibody titers after a primary immunization, which is consistent with previous work[11]. Following an antigenic boost at day 36, all the immunized mice, independent of the vaccine regimen used, responded robustly indicating that they were immunologically primed (Figure 1A).

Because an immune response against the LcrV protein (V antigen) is critical for protection against plague[13,24,25], ELISAs were performed to determine if antibodies produced after immunization with the selected vaccine regimens were specific for the V antigen. All the vaccine formulations evaluated induced similar levels of anti-LcrV antibodies with the exception of the nanoparticle-encapsulated unmodified F1-V group (E_{unmod}), for which the average titer value was below 1,000 (data not shown).

In addition to the quantitative humoral response, antibody quality plays an important role in mounting a protective response against pathogens such as *Y. pestis*[11] and *Streptococcus pneumoniae*[26]. As a measure of quality, antibody avidity was evaluated by assessing binding in the presence of the chaotropic reagent, sodium thiocyanate. Prior to the booster immunization, mice immunized with $S_{αGal} + E_{unmod}$ produced antibodies with high avidity (Figure 1B). Following the booster immunization, the antibody avidity of all immunized mice was significantly enhanced (Figure 1B) with the exception of those receiving the MPLA + $S_{αGal}$ formulation, which already had high avidity antibodies. Moreover, mice immunized with regimens containing αGal-F1-V alone or in conjunction with nanoparticles presented with significantly higher avidity antibodies as compared to antibody from mice immunized with the unmodified F1-V.

Soluble αGal-F1-V + F1-V encapsulated nanoparticles ($S_{αGal} + E_{unmod}$) promoted the development of antigen-specific CD4$^+$ T cell responses. Although humoral immunity is required for protection against plague, evidence suggests that cell-mediated immunity may also be necessary[27,28]. Indeed, CD4$^+$ T helper cells provide B cell help at various stages of the humoral immune response[29,30]. To investigate if our vaccine formulations induced a T cell response, antigen-specific CD4$^+$ T cell proliferation was evaluated via an *in vitro* recall response. Significantly more antigen-specific T cell proliferation was observed in cultures of lymph node cells recovered from mice vaccinated with the $S_{αGal} + E_{unmod}$ formulation as compared to cultures of lymph node cells isolated from mice immunized with any other formulation (Figure 2). CD4$^+$ T cells from mice immunized with either $S_{αGal}$ or S_{unmod} F1-V antigen adjuvanted with MPLA showed no significant increase in proliferation over those from saline controls. Similarly, no difference in recall response was observed for lymph node cells recovered from mice immunized with nanoparticle-encapsulated unmodified (SI = 2.11) or αGal-modified (SI = 1.17) F1-V (data not shown) compared to naïve controls. Of note, the only other vaccine formulation to induce significantly more antigen-specific proliferative CD4$^+$ T cells as compared to naïve control mice was the $S_{αGal}$ alone.

Immunization with the $S_{αGal} + E_{unmod}$ formulation generated antibodies that were more broadly reactive to F1-V peptide epitopes. Many pathogens evade immune system recognition and clearance by eliciting antibody responses against non-protective epitopes or by constantly mutating their antibody binding sites to avoid inhibition via antibodies raised against previous strains. Designing vaccine formulations capable of generating broadly reactive antibodies would prevent pathogen escape and reduce the risk of pandemic spread. To characterize the breadth of the serum antibody reactivity to specific F1-V protein epitopes following vaccination, we examined

Table 1 | Vaccination regimens

Group #	Experimental Group	Soluble F1-V (μg)*	Soluble αGal-F1-V (μg)*	Encapsulated F1-V (μg)*
1	Control-Saline	-----	-----	-----
2	S_{unmod}	5	-----	-----
3	$S_{αGal}$	-----	5	-----
4	$S_{unmod} + E_{unmod}$	2.5	-----	2.5
5	$S_{αGal} + E_{unmod}$	-----	2.5	2.5
6	S_{unmod} + MPLA	5	-----	-----
7	$S_{αGal}$ + MPLA	-----	5	-----

*Quantities indicate the amounts of immunogen delivered to each mouse in the indicated group. S = soluble antigen; E = encapsulated antigen. Subscripts indicate type of F1-V antigen (i.e., unmodified or αGal-modified F1-V) administered per dose. Each mouse was administered 500 μg of 50 : 50 CPTEG : CPH nanoparticles or 10 μg of MPLA in respective treatment formulations. All formulations were administered subcutaneously in a total volume of 100 μL of saline. Following primary immunization with the various vaccine formulations, the mice were then subcutaneously administered with a booster immunization at day 37, comprising 5 μg of unmodified F1-V.
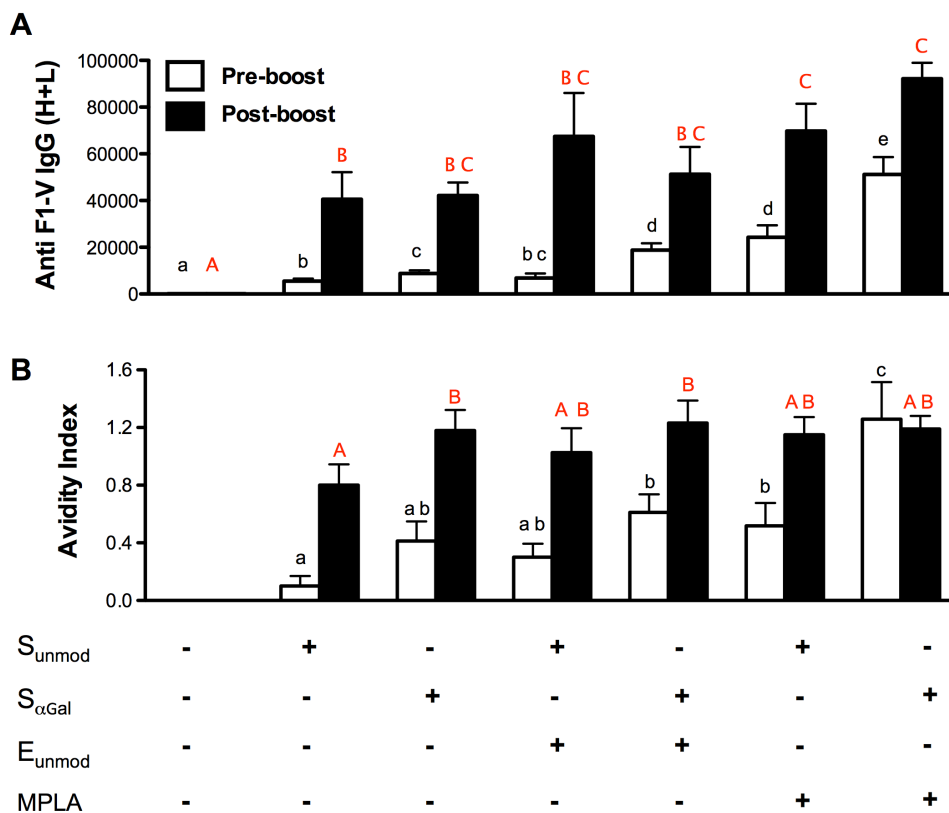
Figure 1 | Soluble αGal-F1-V and F1-V encapsulated nanoparticle formulations synergistically generated a high titer, high avidity antibody response. Mice were subcutaneously immunized with various vaccine formulations and then subcutaneously administered a boost of 5 μg of unmodified F1-V 37 days after immunization. Serum was collected both prior to boost on day 36 (open bar) and after the boost (closed bar) at day 42 and evaluated for (A) F1-V-specific antibody titers via ELISA measuring IgG (H + L) or (B) F1-V-specific antibody avidity using sodium thiocyanate as the chaotropic agent. Data are presented as the mean ± SEM of four independent experiments each consisting of 6–10 mice per group. Letters represent statistical comparisons among groups either pre-boost (smaller case) or post-boost (upper case). Treatments identified with different letters are significantly different from one another (p ≤ 0.05).

antibody binding against two separate panels of overlapping peptides. The first panel of 27 peptides covered the full length of the F1 antigen and the second panel covered the full length of the V antigen (53 peptides). Hierarchical clustering analysis and principal component analysis (PCA) of the generated data matrix enabled identification of immunodominant peptides (Figures 3A and 3B). Of the 27 F1 peptides evaluated, only two (i.e., F1-1 and F1-18) were recognized by sera from all immunized mice. Consistent with previous findings[31], the majority of the anti-F1-V response was directed against the V portion of the protein and, in particular, against six V peptides (i.e., V-2, V-14, V-19, V-20, V-27 and V-44) (Figures 3A and 3B). Of note, removal of these dominant peptides from the data analysis revealed widespread recognition of multiple F1 and V peptides by serum antibodies from mice immunized with the $S_{\alpha Gal}$ + E_{unmod} formulation (Figure 3C, lane 5). In contrast, serum antibodies from mice immunized with F1-V + MPLA showed weak reactivity to the vast majority of the remaining F1-V peptides, indicating that most of the antibodies were directed against the immunodominant epitopes.

The peptide region spanning amino acids 196–225 of LcrV is known to be protective in mice[31,32]. Six of the V peptides in the array, V-32, V-33, V-34, V-35, V-36 and V-37, are located in this region. To evaluate the antibody response in the protective region of the V protein, we evaluated the increase in antibody reactivity over saline controls for these six peptides. Once again, the antibodies from mice immunized with the $S_{\alpha Gal}$ + E_{unmod} formulation demonstrated the greatest recognition with at least a 1.5-fold change for five (i.e., V-32, 33, 35, 36 and 37) of the six peptides (Figure 3D). In contrast, antibodies from the $S_{\alpha Gal}$ + MPLA group reacted strongly with only the

V-33 peptide, while the S_{unmod} + MPLA group showed a 1.5-fold change for only two peptides.

Identification of the lead candidate nanovaccine formulation. PCA was used to perform a composite analysis of the immune response data, including the antibody responses, T cell proliferation, and peptide array data (Supplementary Fig. 3). This analysis enabled simultaneous investigation of the relationships among the multiple variables of the vaccine regimens evaluated in this study, including αGal modification of the F1-V, use of nanoparticles versus MPLA, and amount of soluble versus nanoparticle-encapsulated protein.

Figure 4 shows the results from the PCA. In this figure, the distance along the direction (i.e., down and to the right) of the red arrow indicates enhancement in immunity compared to the saline treatment. Treatments circled together in blue demonstrated similar responses. When the unmodified F1-V antigen was delivered as either soluble protein alone (S_{unmod}) or together with nanoparticles (S_{unmod} + E_{unmod}), the groups were located closer to the saline control in the principal component data space, indicating that the weakest immune response was obtained after vaccination with these regimens. The analysis also indicated that the impact of adding MPLA as an adjuvant is unclear. While adding MPLA to either S_{unmod} or $S_{\alpha Gal}$ increased the distance from the saline control along the PC1 axis, both formulations were located in the top quadrant, indicating similarity to the saline control. The presence of soluble αGal-modified F1-V in the vaccine formulation had the largest impact in terms of significant change from the saline control because the $S_{\alpha Gal}$ and $S_{\alpha Gal}$ + E_{unmod} groups were located in the lower right quadrant.
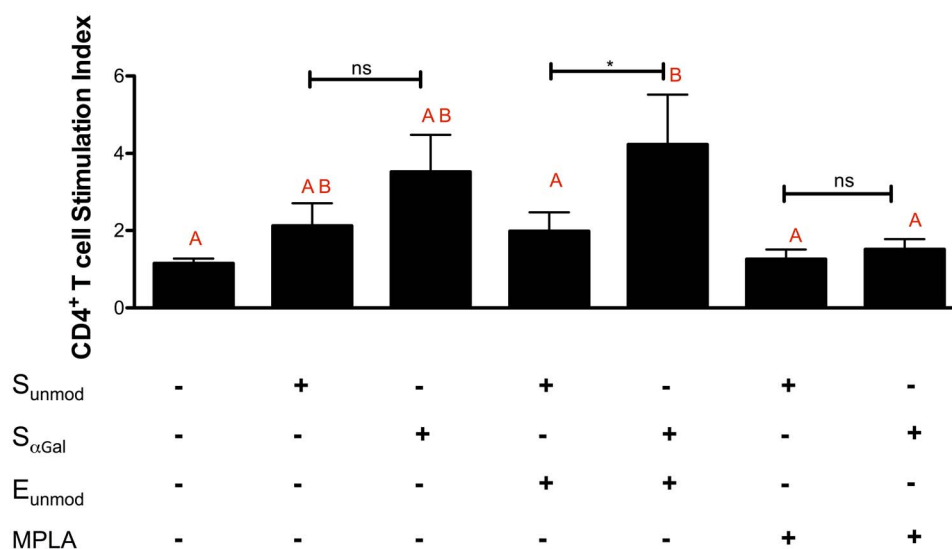
Figure 2 | Soluble αGal-F1-V combined with F1-V encapsulated nanoparticles promoted the development of antigen-specific CD4+ T cell responses. Draining lymph node cells were harvested at d42 post-immunization, labeled with CFSE, cultured with or without 10 μg/mL of F1-V antigen for four days, stained with fluorescent antibodies against CD4, and analyzed by flow cytometry. Stimulation index was calculated by dividing the percentage of CD4+ T cells that proliferated in the presence of F1-V by the percentage of CD4+ T cells that proliferated in the medium alone control. Data are presented as the mean stimulation index ± SEM of two independent experiments each consisting of 6–10 mice per treatment group. Treatments identified with different letters are significantly different from one another ($p \leq 0.05$).

Ultimately, the analysis revealed that $S_{\alpha Gal} + E_{unmod}$ was the lead candidate nanovaccine formulation based on its geometric distance from the saline control along the red arrow.

Discussion

Efficacious vaccines capable of inducing protection against infectious diseases are typically able to do so by mimicking the way in which a naturally occurring infection induces a robust immune response[7,33]. Directing antigen internalization by APCs and sustaining antigen exposure are key elements to augmenting and extending immune stimulation[33,34]. In this work, a systems approach is presented for the rational design of efficacious vaccines by synergistically combining two platforms, αGal modification of the vaccine antigen and amphiphilic nanoparticles with dual functions as vaccine carriers and adjuvants. Informatics analysis validated the synergy provided by this approach by unraveling hidden relationships among multi-dimensional attributes embedded in diverse sets of experimental data and identifying a lead candidate nanovaccine formulation. The use of this systems approach incorporated a holistic vaccine design philosophy by focusing on more than antibody titer (i.e., titer, avidity, breadth of epitope recognition, and CD4 T cell reactivity) and enabled the identification of a formulation that generated a mature, high quality humoral immune response as well as a cell-mediated immune response.

In this work, we demonstrated that vaccine formulations containing soluble αGal-F1-V induced both a high-titer and high quality antibody response (Figure 1A). The induction of endogenous high-titer anti-αGal antibodies promotes opsonization of αGal-modified antigens[15,35] that would facilitate the formation of immune complexes that would enhance antigen binding to follicular dendritic cells (FDCs) for antigen presentation to B cells[36,37] and antigen uptake and presentation by APCs to enhance T cell responses via several mechanisms, including complement activation and Fc receptor (FcR)-mediated endocytosis[16,18]. Moreover, the formation of these antigen-antibody immune complexes may potentially lead to prolonged recycling of antigen on the surface of FDCs[37], CD19/CD21-mediated B cell activation[38,39] and accelerated memory B cell development, germinal center formation, and antibody affinity maturation[40,41]. Despite an earlier report indicating that complement

receptors are not required for the development of antibody responses following immunization with certain αGal modified antigens[19], more recent work clearly demonstrates that other components of the complement cascade are critical for antigen deposition on the surface of FDCs, activation of germinal center B cells, and the subsequent maturation of antigen-specific B cell response[37,42,43]. Long-term retention of these immune complexes on FDCs and extended antigen exposure to B cells are likely mechanisms by which complement and preexisting antibody can contribute to productive primary and secondary B cell responses. Moreover, complement activation promotes the release of various chemotactic factors that induce APC migration and uptake of αGal modified antigen by Fc receptor-mediated endocytosis[44,45]. Collectively, these immune complex-mediated mechanisms may explain how our nanovaccines containing αGal-F1-V induced a high-titer, high quality antibody response characterized by a greater breadth of epitope recognition and F1-V-specific CD4+ T cell responses when compared to vaccine regimen that did not contain αGal-F1-V.

Antibody production was significantly enhanced when soluble αGal-F1-V was delivered together with nanoparticle-encapsulated unmodified F1-V (Figure 1A). This finding demonstrates the value of the systems approach to vaccine design by effectively combining the correct antigen and adjuvant platforms. Specifically, the efficacy of including soluble αGal-modified antigen along with encapsulated unmodified antigen may be attributable to the *in situ* generation of F1-V immune complexes. Indeed, immune complexes are known to significantly influence the rapidity, intensity, and specificity of the subsequent antibody response against the target antigen[40]. The enhanced immune effects promoted by immune complexes are associated with affinity maturation of B cells[41] and may result in the production of more avid antibodies. This may explain why antibodies with higher avidity were obtained following immunization with αGal-modified F1-V (Figure 1B). In parallel, it is also known that continuous antigen exposure is critical for developing high avidity antibodies during affinity maturation[46]. In the present work, antibodies with higher avidity were produced after immunization with formulations containing both soluble and nanoparticle-encapsulated antigen (Figure 1B), demonstrating the role of the nanoparticles in providing continual antigen release. Previous work from our
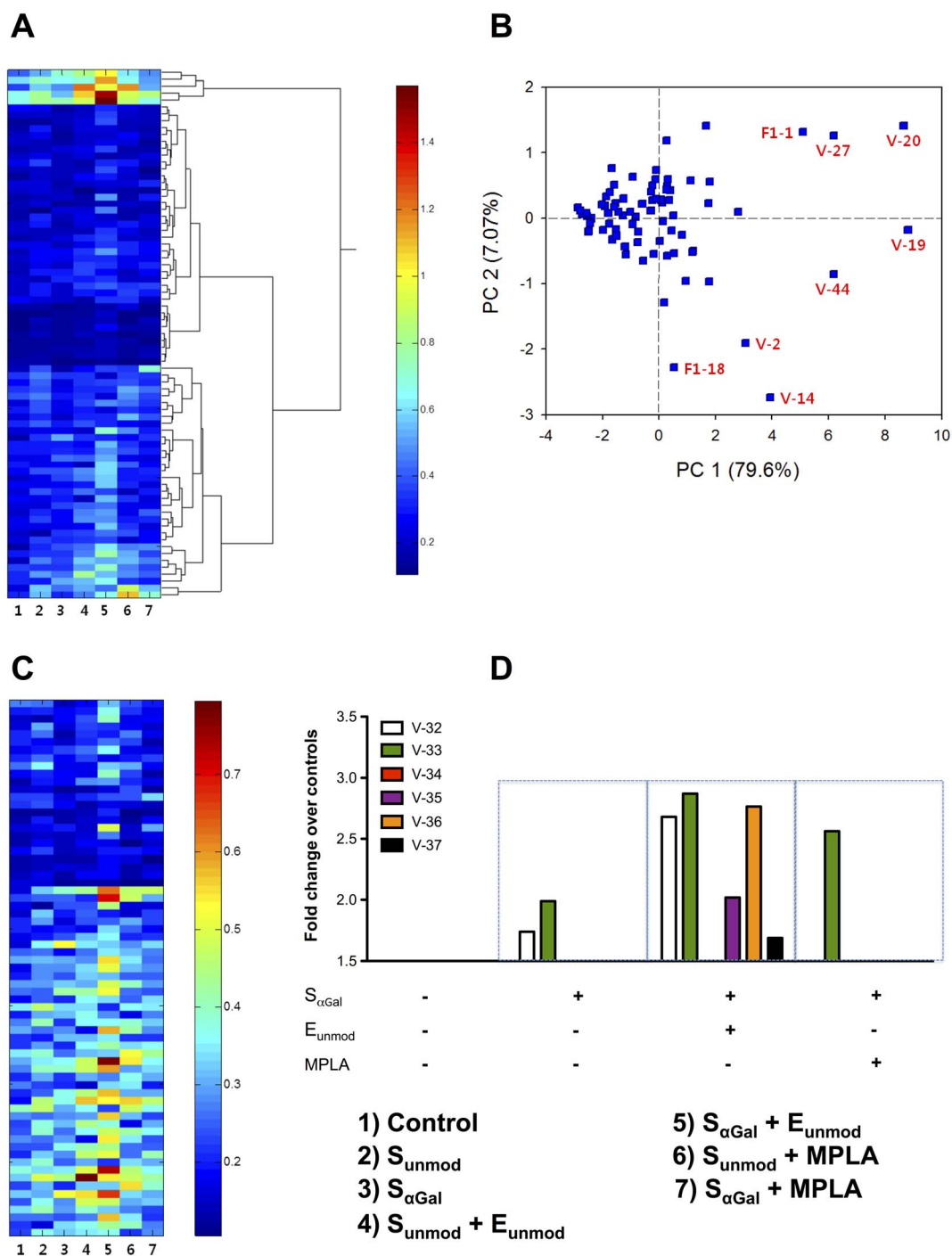
Figure 3 | Antibodies generated by immunization with the S$_{\alpha Gal}$ + E$_{unmod}$ formulation were more broadly reactive to F1-V peptide epitopes. Differential epitope recognition by antibodies elicited during immunization with the various vaccine formulations was determined using a peptide array for both F1 and V antigens from *Y. pestis*. Mice were immunized with the vaccine regimens described in Table 1 and administered an antigenic boost of 5 μg of unmodified F1-V 37 days after immunization. (A) Heat map depicting recognition of the 80 peptides via mouse sera after hierarchical clustering analysis implementation, which allows for grouping of peptides demonstrating a relatively higher response than others. (B) Principal component analysis (PCA) of peptide arrays corroborates as outliers the same set of peptides identified by clustering analysis. The plot maps out high dimensional correlations, permitting identification of significant responders from the peptide array data. (C) Broader peptide recognition by specific vaccination groups is illustrated by a heat map, depicting antibody responses elicited via different vaccination regimens against the set of peptides not identified as outliers by the clustering analysis. (D) The increase in antibody reactivity over saline controls was used to determine antibody response against the protective region of the V protein (represented by peptides V-32, V-33, V-34, V-35, V-36 and V-37). For (A) and (C), peptides for which greater immunoreactivity was observed for specific immunization groups are presented as red, yellow, or light blue while vaccination treatments are represented by numbers identifying each of the columns for the heat map: 1) control, 2) S$_{unmod}$, 3) S$_{\alpha Gal}$, 4) S$_{unmod}$ + E$_{unmod}$, 5) S$_{\alpha Gal}$ + E$_{unmod}$, 6) S$_{unmod}$ + MPLA, and 7) S$_{\alpha Gal}$ + MPLA. Data are the average measurements for three pooled serum samples per vaccination group (each of the pools contained samples from three or four mice).
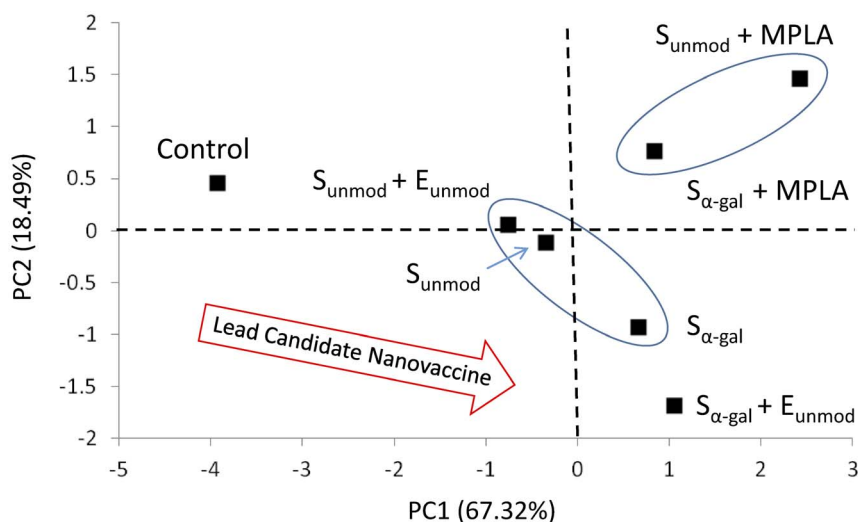
Figure 4 | Informatics analysis identified lead candidate vaccine formulation. PCA scores plot of various vaccine regimens. The plot maps out high dimensional correlations, permitting the tracking of the relative influences of varying the vaccine formulation. The distance along the direction of the red arrow (i.e., down and to the right) indicates enhancement in immunity following vaccination, and groups that are circled together in blue demonstrated similar responses.

laboratories has shown that amphiphilic 50:50 CPTEG:CPH nanoparticles were internalized by APCs at a slower rate than hydrophobic CPH:SA nanoparticles[7,12]. Moreover, the amphiphilic nanoparticles persisted longer after subcutaneous administration[47]. This depot effect, in combination with slow antigen release due to nanoparticle degradation, likely allows for the extended presence of antigen *in vivo* and results in more avid antibodies.

In addition to enhancing antibody production, the $S_{\alpha Gal} + E_{unmod}$ formulation also induced the greatest F1-V specific CD4+ T cell proliferation when compared to all other vaccine regimens used in this study (Figure 2). This enhanced T cell response may be a consequence of improved FcR-mediated uptake of αGal-F1-V immune complexes and presentation via APCs. The cross-presentation pathway accessed by antigens acquired endocytically through FcRs has been previously reported to enhance antigen-specific T cell responses, thereby linking the preexisting anti-αGal antibody response with enhanced cellular immunity[48].

Preservation of antigenic epitopes during vaccine delivery is essential for generating a protective immune response[31]. In this regard, the amphiphilic 50:50 CPTEG:CPH particles have been shown previously to release stable F1-V antigen[5], which may translate into epitope preservation *in vivo*. Applying informatics analysis tools to peptide array data of the F1-V protein revealed two F1 and six V immunodominant peptides. An amino acid region that correlates with protection from lethal challenge following passive immunotherapy is located at the amino-terminal end of F1[23]. It is well known that the V antigen is an effector protein, and some of its epitopes are important for activation of the contact-dependent Type III secretion system during infection[24,31,49–52]. The LcrV region spanning amino acids 135–275[53], more specifically amino acids 196–225[54], is the dominant epitope for antibody-mediated protection against plague. Here, we demonstrated that the $S_{\alpha Gal} + E_{unmod}$ vaccine formulation not only elicited more avid antibodies specific for peptides encompassing the protective region (Figure 3D), but also elicited antibodies recognizing a more diverse array of the remaining peptides, resulting in a broader epitope spread. Previous work has shown that antigen-antibody complexes may modulate the humoral immune response by masking dominant epitopes, improving germinal center formation, inducing somatic hypermutations, and promoting changes in antigen processing[40]. Furthermore, alterations in the sequences of T cell epitopes are known to modulate the diversity and spectrum of the resultant antibody response[40]. The combination of F1-V immune complexes and continued release of antigen from nanoparticles may facilitate the engagement of multiple B cells with different receptor specificities that contributed to the diverse epitope recognition that was observed in this study. Induction of an antibody repertoire capable of broad epitope recognition is pivotal to developing efficacious vaccines against influenza and HIV that constantly mutate epitopes to evade the immune response[55].

Figure 5 shows how the systems approach proposed herein could be used to enhance vaccine performance due to a synergistic combination of several mechanisms provided by each of the platforms that resulted in the identification of a lead nanovaccine candidate. When translating these results to humans, the use of αGal-modified immunogens would result in the formation of antigen-antibody immune complexes that would promote CD19/CD21-mediated B cell activation, accelerate memory B cell development, germinal center formation, and antibody affinity maturation. The use of antigen-loaded amphiphilic nanoparticles would provide sustained release of the antigen, resulting in antigen persistence *in vivo* and more avid antibodies. The rational choice of the amphiphilic nanoparticles enables preservation of antigenic structure and function, which results in enhanced breadth of epitope recognition by antibodies. Finally, the combination of αGal-modified antigen and amphiphilic nanoparticles would further enhance APC-T cell interactions, leading to a more robust cell-mediated immune response, which is an important correlate of protective immunity against several pathogens[56,57]. In contrast to conventional methods that "mix and match" off-the-shelf antigens and adjuvants, the systems approach for judicious and concomitant design of novel antigen and adjuvant technologies that work synergistically can lead to rational design of efficacious vaccines. This more holistic approach to vaccine design provides a new paradigm for development of next generation vaccines against emerging and re-emerging pathogens.

Methods

Antigenic modification of F1-V. Recombinant F1-V obtained from NIH Biodefense and Emerging Infections Research Resources Repository (BEI, Manassas, VA) was modified by chemical addition of αGal epitopes at lysine residues. Chemical addition of αGal epitopes was performed at BioProtection Systems Corporation, a subsidiary of NewLink Genetics Corporation (Ames, IA), using an efficient chemo-enzymatic synthesis of the αGal trisaccharide and conjugation[58]. The modified F1-V was characterized by SDS-PAGE and western blot. αGal-modified and unmodified F1-V were loaded onto 12% Tris-Glycine pre-cast gels (Bio-Rad Laboratories, Richmond,
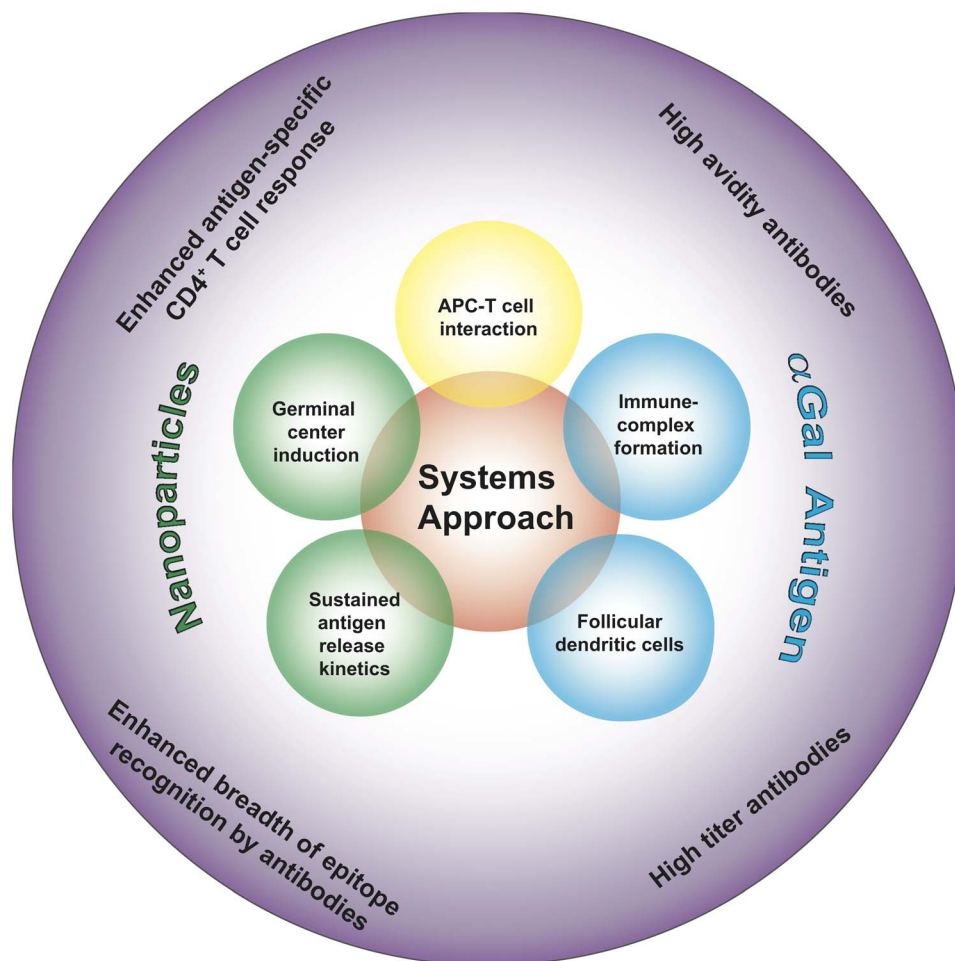
Figure 5 | Cartoon representation of the systems approach describing a new paradigm for designing next generation vaccines against emerging and re-emerging pathogens. Specific immune mechanisms are targeted by either the αGal-antigen (blue bubbles), amphiphilic polyanhydride nanoparticles (green bubbles) or both platforms (yellow bubble). As a result of the synergistic activation of such mechanisms, an augmented and extended antigen-specific immune response was obtained (purple bubble).

CA), run for 90 min at 100 V, and electro-transferred to a PVDF membrane for 1 h at 120 V. The membrane was then blocked with 1% fish skin gelatin in Tris-buffered saline with Tween-20 (TBST) buffer overnight at 4°C. The following day, membranes were washed three times in TBST and incubated with αGal positive antisera diluted 1:1,000 in TBST for 2 h. The membrane was then washed and incubated with alkaline phosphatase conjugated goat anti-mouse IgG diluted in TBST (1:1,000) for 2 h. Bands were visualized with SIGMA FAST Red TR/Naphthol AS-MX Phosphate tablets (Sigma Aldrich, St. Louis, MO). Lane 3 in Supplementary Fig. 1 shows that only bands corresponding to the αGal-F1-V protein were present, further confirming the successful attachment of αGal epitopes to the protein.

Polymer synthesis and characterization. Synthesis of 1,6-bis(*p*-carboxyphenoxy)hexane (CPH) and 1,8-bis(*p*-carboxyphenoxy)-3,6-dioxaoctane (CPTEG) diacids was performed as described previously[8]. Proton NMR and gel permeation chromatography were utilized to confirm chemical structure and to measure molecular weight, respectively. The 50:50 CPTEG:CPH copolymer had an average molecular weight of 8,500 Da and a polydispersity index of 1.70, consistent with previous work[5,8].

Nanoparticle synthesis and characterization. F1-V encapsulated nanoparticles were synthesized by the anti-solvent nanoencapsulation method reported previously[11,12]. Scanning electron microscopy (SEM, JEOL 840A, JEOL Ltd., Tokyo, Japan) and quasi-elastic light scattering (QELS, Zetasizer Nano, Malvern Instruments Ltd., Worchester, UK) were employed to characterize particle morphology and size, respectively. Photomicrographs of F1-V and αGal-F1-V loaded 50:50 CPTEG:CPH nanoparticles (not shown) showed similar spherical morphology and size (147 ± 23 nm for F1-V loaded particles versus 169 ± 16 nm for αGal-F1-V loaded particles), which was consistent with QELS analysis and with particle morphology and sizes observed in previous studies[6,7,11].

Mice. The α1,3GT gene knockout (KO) mouse model on a BALB/c background was used to evaluate immune responses to αGal and mimic human immunity to this epitope. Mice were obtained from BioProtection Systems Corporation (Ames, IA) and housed under specific pathogen-free conditions where all bedding, caging, and feed were sterilized prior to use. All animal procedures were conducted with the approval of the Iowa State University Institutional Animal Care and Use Committee and were in full compliance with the Committee's guidelines. Three intraperitoneal injections of rabbit red blood cells (RRBCs; 3×10^8 RRBCs/injection) were administered at 14-day intervals to induce production of anti-αGal antibodies. All RRBC injections were administered prior to immunization with any vaccine formulations. Seven days after the final RRBC injection, anti-αGal specific serum antibodies were quantified via ELISA. Only mice with serum optical density values ($OD_{405 nm}$) higher than 5X background (PBS) were used in the study; animals were distributed randomly across the different immunization groups.

Vaccination regimens. Mice were immunized subcutaneously with the regimens described in Table 1 by suspension in pyrogen-free saline in a volume of 100 μL. Monophosphoryl lipid A (MPLA) from *Salmonella Enterica* serotype minnesota Re 595 (Sigma) was used as a control adjuvant at a dose of 10 μg per mouse. A booster immunization of 5 μg of unmodified F1-V was subcutaneously administered to all mice 37 days after primary immunization. Blood samples were collected from the left saphenous vein prior to boost (pre-boost) at day 36. Five days after booster immunization (day 42), mice were euthanized and serum collected via cardiac puncture (post-boost). Experiments were performed in quadriplicate with an average of 6–8 mice per group in each experiment.

Anti-F1-V and anti-LcrV titers. An ELISA method was adapted from a previously published protocol[11,12]. Briefly, microtiter plates were coated overnight with 0.5 μg/mL of F1-V or LcrV (BEI) in phosphate buffered saline (PBS), blocked with 2% (w/v) gelatin for 2 h and washed with PBS containing Tween-20 (PBS-T). Sera samples were serially diluted two fold in PBS-T with 1% (v/v) normal goat serum, and incubated overnight at 4°C. After washing, plates were reacted with alkaline phosphatase (AP)-conjugated goat anti-mouse IgG (H&L) (Jackson ImmunoResearch, West Grove, PA) at room temperature for 2 h. Finally, plates were

allowed to react for 20 min at room temperature with phosphatase substrate (Sigma Aldrich). Optical density (OD) of each well was measured at 405 nm. Endpoint titers were defined as the highest dilution with an OD value of at least 0.2.

Antibody avidity assay. Antibody avidity analysis was performed as described previously[11,12] by coating plates overnight with 0.5 µg/mL F1-V in PBS. Changes in OD were measured at 405 nm using a spectrophotometer. Avidity index was defined as the concentration of NaSCN necessary to reduce the OD by 50% compared to the wells treated with 0.1 M sodium phosphate.

In vitro CD4$^+$ T cell proliferation assay. Antigen specific recall responses were measured as described elsewhere[59]. Briefly, a single cell suspension of draining lymph nodes (brachial and axial) was prepared using a glass tissue homogenizer. Cells were stained with carboxyfluorescein diacetate succinimidyl ester (CFSE) dye, plated at a density of 2.5×10^5 cells per well and cultured either in the presence or absence of 10 µg/mL F1-V for four days at 37°C, 5% CO_2. Cells cultured in medium alone were used as negative controls. Following the incubation, cells were harvested, washed, stained with a PE-Cy7 labeled anti-CD4 antibody, fixed, and acquired on a Becton-Dickinson FACSCanto™ flow cytometer (San Jose, CA). Data were analyzed using FlowJo software (TreeStar Inc., Ashland, OR). Data are presented as a stimulation index, which was calculated by dividing the percentage of CD4$^+$ T cells that proliferated in the presence of F1-V by the percentage of CD4$^+$ T cells that proliferated in the medium alone control.

Statistical analysis. Statistical analysis was performed using JMP® software (SAS Institute, Cary, NC). For comparisons of multiple vaccine formulations, data were analyzed using Tukey's honestly significant difference (HSD) with logarithmic transformation. Differences were considered significant when $p < 0.05$.

Epitope mapping by peptide arrays. Two sets of overlapping peptides, one panel covering the full length of the F1 antigen (27 peptides) and the other covering the full length of the V antigen (53 peptides), were obtained from BEI. Immunlon 2 HB 96-well plates were coated with the peptides (5 µg/mL) and incubated overnight at 4°C. Plates were blocked for 2 h at room temperature with 2.5% skim milk in PBS-T. Sera samples were diluted 1 : 200 and incubated overnight at 4°C. After three washing steps with PBS-T, AP-conjugated goat anti-mouse IgG(H&L) at a 1 : 1,000 dilution was added. Plates were allowed to react for 2 h with the phosphatase substrate buffer described before and changes in OD were determined at 405 nm.

Informatics analysis. *Hierarchical clustering.* Cluster analysis was used to identify the peptides for which significantly enhanced immunoreactivity was observed for specific immunization groups and to compare the responses of the various vaccine formulations. In this method, the similarity between observations was assessed according to their relative proximity in the data space. Starting from separate data points in the parameter space, R^N (N = 10 for the comparison of 80 peptides, and N = 80 for 10 different immunization groups), the Euclidean distance, d_E, was calculated to define clusters according to the following equation:

$$d_E = \sqrt{\sum_{i=1}^{N} (x_i - y_i)^2}$$

The artificial color-coding of a heat map indicated the relative distance among the data, and the corresponding tree structure, referred to as a dendrogram, showed the hierarchical grouping.

PCA. PCA was used to mathematically capture differences in properties between various vaccine formulations. PCA finds "hidden" relationships by describing the data in a form that reduces inter-correlations. The inputs into the analysis were the conditions (i.e., antigens and their various formulations) and the outputs were the biological responses (i.e., titer, avidity, epitope recognition). The data was decomposed into two plots: the scores plot (Figure 4), which described the conditions and the loadings plot (Supplementary Figure 3), which described the responses. The degree of correlation in the results was indicated by proximity; that is, two points with similar PC values were highly correlated while two points with different PC values were less correlated.

To compare similarity of conditions to the control, a line drawn through the control and the origin described the direction of the control, while any distance off this line was unrelated to the control. The projection (perpendicular) of the various points onto this line described similarity to the control.

1. Wilson-Welder, J. H. *et al.* Vaccine adjuvants: Current challenges and future approaches. *J Pharm Sci* **98**, 1278–1316 (2009).
2. Feng, L. *et al.* Pharmaceutical and immunological evaluation of a single-dose hepatitis B vaccine using PLGA microspheres. *J Cont Rel* **112**, 35–42 (2006).
3. Phanse, Y. *et al.* Functionalization of polyanhydride microparticles with di-mannose influences uptake by and intracellular fate within dendritic cells. *Acta Biomater* **9**, 8902–8909 (2013).
4. Petersen, L. K., Phanse, Y., Ramer-Tait, A. E., Wannemuehler, M. J. & Narasimhan, B. Amphiphilic polyanhydride nanoparticles stabilize *Bacillus anthracis* protective antigen. *Mol Pharm* **9**, 874–882 (2012).
5. Carrillo-Conde, B. *et al.* Amphipilic polyanhydrides for stabilization of *Yersinia pestis* antigens. *Acta Biomater* **6**, 3110–3119 (2010).
6. Carrillo-Conde, B. *et al.* Mannose-functionalized "pathogen-like" polyanhydride nanoparticles target C-type lectin receptors on dendritic cells. *Mol Pharm* **8**, 1877–1886 (2011).
7. Petersen, L. K. *et al.* Activation of innate immune responses in a pathogen-mimicking manner by amphiphilic polyanhydride nanoparticle adjuvants. *Biomaterials* **32**, 6815–6822 (2011).
8. Torres, M. P., Determan, A. S., Anderson, G. L., Mallapragada, S. K. & Narasimhan, B. Amphiphilic polyanhydrides for protein stabilization and release. *Biomaterials* **28**, 108–116 (2006).
9. Torres, M. P. *et al.* Polyanhydride microparticles enhance dendritic cell antigen presentation and activation. *Acta Biomater* **7**, 2857–2864 (2011).
10. Ulery, B. D. *et al.* Polymer chemistry influences monocytic uptake of polyanhydride nanospheres. *Pharm Res* **26**, 683–690 (2008).
11. Ulery, B. D. *et al.* Design of protective single-dose intranasal nanoparticle-based vaccine platform for respiratory infectious diseases. *PLoS One* **6**, e17642 (2010).
12. Ulery, B. D. *et al.* Rational design of pathogen-mimicking amphiphilic materials as nanoadjuvants. *Sci Rep* **1**, 198 (2011).
13. Anderson, G. W. J., Heath, D. G., Bolt, C. R., Welkos, S. L. & Friedlander, A. M. Short- and long-term efficacy of sinlge-dose subunit vaccines agaisnt *Yersinia pestis* in mice. *Am J Trop Med Hyg* **58**, 793–799 (1998).
14. Galili, U., Rachmilewitz, E. A., Peleg, A. & Flechner, I. A unique natural human IgG antibody with anti-α-Galactosyl specificity. *J Exp Med* **160**, 1519–1531 (1984).
15. Galili, U. *et al.* Evolution and pathophysiology of the human natural anti-α-Galactosyl IgG (anti-Gal) antibody. *Springer Semin Immunopathol* **15**, 155–171 (1993).
16. Abdel-Motal, U. M., Guay, H. M., Wigglesworth, K., Welsh, R. M. & Galili, U. Immunogenicity of influenza virus vaccine is increased by anti-Gal-mediated targeting to antigen-presenting cells. *J Virol* **81**, 9131–9141 (2007).
17. Abdel-Motal, U. M., Wigglesworth, K. & Galili, U. Mechanism for increased immunogenicity of vaccines that form in vivo immune complexes with the natural anti-Gal antibody. *Vaccine* **27**, 3072–3082 (2009).
18. Abdel-Motal, U. M. *et al.* Increased immunogenicity of HIV-1 p24 and gp120 following immunization with gp120/p24 fusion protein vaccine expressing alpha-gal epitopes. *Vaccine* **28**, 1758–1765 (2010).
19. Benatuil, L. *et al.* The influence of natural antibody specificity on antigen immunogenicity. *Eur J of Immunol* **35**, 2638–2647 (2005).
20. Mandell, R. B. *et al.* The αGal HyperAcute® technology: enhancing immunogenicity of antiviral vaccines by exploiting the natural aGal-mediated zoonotic blockade. *Zoonoses Public Hlth* **56**, 407–428 (2008).
21. Airhart, C. L. *et al.* Lipid A mimetics are potent adjuvants for an intranasal pneumonic plague vaccine. *Vaccine* **26**, 5554–5561 (2008).
22. Elvin, S. J. *et al.* Protection against bubonic and pneumonic plague with a single dose microencapsulated sub-unit vaccine. *Vaccine* **24**, 4433–4439 (2006).
23. Xiao, X. *et al.* Human anti-plague monoclonal antibodies protect mice from *Yersinia pestis* in a bubonic plague model. *PLoS One* **5**, e13047 (2010).
24. Chiuchiolo, M. J. *et al.* Protective immunity against respiratory tract challenge with *Yersinia pestis* in mice immunized with an adenovirus-based vaccine vector expressing V antigen. *J Infect Dis* **194**, 1249–1257 (2006).
25. Do, Y. *et al.* Targeting of LcrV virulence protein from *Yersinia pestis* to dendritic cells protects mice against pneumonic plague. *Eur J Immunol* **40**, 2791–2796 (2010).
26. Lee, L. H., Frasch, C. E., Falk, L. A., Klein, D. L. & Deal, C. D. Correlates of immunity for pneumococcal conjugate vaccines. *Vaccine* **21**, 2190–2196 (2003).
27. Philipovskiy, A. V. & Smiley, S. T. Vaccination with live *Yersinia pestis* primes CD4 and CD8 T cells that synergistically protect against lethal pulmonary *Y. pestis* infection. *Infect Immun* **75**, 878–885 (2007).
28. Smiley, S. T. Cell-mediated defense against *Yersinia pestis* infection. *Adv Exp Med Biol* **603**, 376–386 (2007).
29. Gourley, T. S., Wherry, E. J., Masopust, D. & Ahmed, R. Generation and maintenance of immunological memory. *Semin Immunol* **16**, 323–333 (2004).
30. Sallusto, F. & Lanzavecchia, A. Heterogeneity of CD4$^+$ memory T cells: functional modules for tailored immunity. *Eur J Immunol* **39**, 2076–2082 (2009).
31. Hill, J., Leary, S. E. C., Griffin, K. T., Williamson, E. D. & Tiiball, R. W. Regions of *Yersinia pestis* V antigen that contribute to protection against plague idenfitied by passive and active immunization. *Infect Immun* **65**, 4476–4482 (1997).
32. Motin, V. L., Nakajima, R., Smirnov, G. B. & Brubaker, R. Passive immunity to *Yersinia* mediated by anti-recombinant V antigen and protein A-V antigen fusion peptide. *Infect Immun* **62**, 4192–4201 (1994).
33. Zepp, F. Principles of vacine design-Lessons from nature. *Vaccine* **28**, C14–24 (2010).
34. Williamson, E. D. *et al.* Local and systemic immune response to a microencapsulated sub-unit vaccine for plague. *Vaccine* **14**, 1613–1619 (1996).
35. Galili, U. *et al.* Enhancement of antigen presentation of influenza virus hemagglutinin by the natural human anti-Gal antibody. *Vaccine* **14**, 321–328 (1996).
36. Gonzalez, S. F., Pitcher, L. A., Mempel, T., Schuerpf, F. & Carroll, M. C. B cell acquisition of antigen in vivo. *Curr Opin Immunol* **21**, 251–257 (2009).

37. Heesters, B. A. *et al.* Endocytosis and recycling of immune complexes by follicular dendritic cells enhances B cell antigen binding and activation. *Immunity* **38**, 1164–1175 (2013).

38. Cherukuri, A., Cheng, P. C. & Pierce, S. K. The role of the CD19/CD21 complex in B cell processing and presentation of complement-tagged antigens. *J Immunol* **167** (2001).

39. Goins, C. L., Chappell, C. P., Shashidharamurthy, R., Selvaraj, P. & Jacob, J. Immune complex-mediated enhancement of secondary antibody responses. *J Immunol* **184**, 6293–6298 (2010).

40. Brady, L. J. Antibody-mediated immunomodulation: a strategy to improve host responses against microbial antigens. *Infect Immun* **73**, 671–678 (2005).

41. Kunkl, A. & Klaus, G. G. The generation of memory cells, IV. Immunization with antigen-antibody complexes accelerates the development of B-memory cells, the formation of germinal centres and the maturation of antibody affinity in the secondary response. *Immunol* **43**, 371–378 (1981).

42. Donius, L. R., Handy, J. M., Weis, J. J. & Weis, J. H. Optimal germinal center B cell activation and T-dependent antibody responses require expression of the mouse complement receptor Cr1. *J Immunol* **191**, 434–447 (2013).

43. Roozendaal, R. & Carroll, M. C. Complement receptors CD21 and CD35 in humoral immunity. *Immunol Rev* **219**, 157–166 (2007).

44. Galili, U., Wigglesworth, K. & Abdel-Motal, U. M. Intratumoral injection of alpha-gal glycolipids induces xenograft-like destruction and conversion of lesions into endogenous vaccines. *J Immunol* **178**, 4676–4687 (2007).

45. Galili, U. α1,3Galactosyltransferase knockout pigs produce the natural anti-Gal antibody and simulate the evolutionary appearance of this antibody in primates. *Xenotransplantation* **20**, 267–276 (2013).

46. Eyles, J. E. *et al.* Immunisation against plague by transcutaneous and intradermal application of subunit antigens. *Vaccine* **22**, 4365–4373 (2004).

47. Huntimer, L. *et al.* Evaluation of biocompatibility and administration site reactogenicity of polyanhydride-particle-based platforms for vaccine delivery. *Adv Health Mater* **2**, 369–378 (2013).

48. Rafit, K., Bergtold, A. & Clynes, R. Immune complex-mediated antigen presentation induces tumor immunity. *J Clin Invest* **110**, 71–79 (2002).

49. Powell, B. S. *et al.* Design and testing for a nontagged F1-V fusion protein as vaccine antigen against bubonic and pneumonic plague. *Biotechnol Prog* **21**, 1490–1510 (2005).

50. Pullen, J. K., Anderson, G. W., Welkos, S. L. & Friedlander, A. M. Analysis of the *Yersinia pestis* V protein for the presence of linear antibody epitopes. *Infect Immun* **66**, 521–527 (1998).

51. Titball, R. W. & Williamson, E. D. Vaccination against bubonic and pneumonic plague. *Vaccine* **19**, 4175–4184 (2001).

52. Williamson, E. D. *et al.* Human immune response to a plague vaccine comprising recombinant F1 and V antigens. *Infect Immun* **73**, 3598–3608 (2005).

53. Vernazza, C. *et al.* Small protective fragments of the *Yersinia pestis* V antigen. *Vaccine* **27**, 2775–2780 (2009).

54. Quenee, L. E. *et al.* Amino acid residues 196–225 of LcrV represent a plague protective epitope. *Vaccine* **28**, 1870–1876 (2010).

55. Du, S. X. *et al.* A directed molecular evolution approach to improved immunogenicity of the HIV-1 envelope glycoprotein. *PLoS One* **6**, e20927 (2011).

56. Thakur, A., Pedersen, L. E. & Jungersen, G. Immune markers and correlates of protection for vaccine induced immune responses. *Vaccine* **30**, 4907–492 (2012).

57. Fletcher, H. A. Correlates of immune protection from tuberculosis. *Curr Mol Med* **7**, 319–325 (2007).

58. Naicker, K. P., Li, H., Heredia, A., Song, H. & Wang, L. X. Design and synthesis of alpha Gal-conjugated peptide T20 as novel antiviral agent for HIV-immunotargeting. *Org Biomol Chem* **2**, 660–664 (2004).

59. Ramer, A. E., Vanloubbeeck, Y. F. & Jones, D. E. Antigen-responsive CD4^{+} T cells from C3H mice chronically infected with Leishmania amazonensis are impaired in the transition to an effector phenotype. *Infect Immun* **74**, 1547–1554 (2006).

Acknowledgments

Author contributions

Y.P. and B.C.C. performed the experiments. R.F. and R.M. developed the experimental plan with respect to the use of α-GT KO mice to model a human immune response and performed F1-V modification with αGal epitopes. M.J.W., B.N., A.E.R., B.C.C. and Y.P. designed the experiments and analyzed the data. S.B., C.S.K. and K.R. performed informatics analysis. B.C.C., Y.P., A.E.R., M.J.W. and B.N. prepared the manuscript.

Additional information